Hole dynamics in a strongly correlated two-dimensional spin background

H. Fehske, V. Waas, H. Röder,* and H. Büttner
Physikalisches Institut, Universität Bayreuth, D-8580 Bayreuth, Germany
(Received 24 April 1991)

In this paper we present results of finite-lattice studies of the t-J and the t-t'-J model for 18 (20) sites with up to 4 (2) holes. A modified Lanczos algorithm allowed for the classification of the ground state according to total spin S. In the one-hole sector we find evidence for the existence of hole pockets. We calculate the effective quasiparticle band and show qualitative differences between the t-J and t-t'-J model for $J \gtrsim 0.2$. As U increases we notice a substantial band narrowing, which is maximal at the Nagaoka transition, accompanied by S-level crossings rendering a quasiparticle description difficult. In the high-doping regime we present hole binding energies for up to six holes for the t-J model. Evidence for phase separation is only found for $J > t$. We also studied the magnetic structure of the ground state on the 18-site lattice in the limit $J = 0$. We present a complete ground-state classification for all numbers of holes N_h and find $S = S_{\max}$ at quarter filling in addition to the Nagaoka case.

I. INTRODUCTION

Superconductivity in the high-T_c materials[1] and the considerable activity in trying to explain this phenomenon focuses renewed interest on the physics of strongly correlated fermion systems. Most of the high-T_c superconductors are perovskite-type layer oxides and it now seems generally accepted that their relevant electronic properties are determined by strong correlations between the induced charge carriers (holes or electrons) and the antiferromagnetic spin background realized in the undoped CuO_2 planes of the insulating parent compounds, such as La_2CuO_4 or Nd_2CuO_4. The clear separation of spin and charge degrees of freedom (~ 2 eV; cf. Ref. 2) as well as the size of the ordered magnetic moment in the undoped case lead to a local description of the Cu^{2+} spins in terms of an isotropic Heisenberg model. Upon doping, the Cu^{2+} spins do not form a separated quantum liquid, but are an essential part of the then superconducting quantum liquid as emphasized by Rice,[3,4] among others, for the case of dominating $Cu_{3d_{x^2-y^2}}$-$O_{2p_{x,y}}$ hybridization. It is an open question whether this strongly correlated quantum liquid can be described in the normal state in terms of a conventional Landau Fermi-liquid theory.

Microscopic models for high-T_c superconductivity should therefore incorporate the hopping of charge-carrier holes (t) and antiferromagnetic exchange (J) between spins of neighboring Cu sites as the relevant degrees of freedom. From the outset of the theoretical development Anderson[5] proposed the two-dimensional Hubbard model with large on-site Coulomb interaction U and close to half-filling as a starting point for a theoretical description, at least for the low-lying excitations in the normal phase. The Hubbard model, and even more the t-J model[6,7] (derived for the limit $U \gg t$) have since been studied intensively. Because of the failure of usual perturbation-theory methods in the strong-coupling regime, sophisticated mean-field theories, for example, slave-boson or slave-fermion methods[8] and numerical techniques like exact diagonalizations[9–16] and quantum Monte Carlo simulations,[17,18] were used for a systematic study of these systems.

In this paper we present an exhaustive examination of the ground-state properties of the Hubbard model in the strong-coupling limit for finite clusters of up to 20 sites with various numbers of holes. In Sec. II we briefly describe the model Hamiltonian and the numerical methods for diagonalizing it on finite lattices. In Sec. III A we focus on the ground state of a single mobile vacancy in an antiferromagnetic background. We determine the energy dispersion $E(\mathbf{K},S)$ for total spin S for both the t-J and t-t'-J models as a function of the Coulomb interaction. Here we also discuss the possible existence of a pocketlike Fermi surface, the position of the momentum of the hole,[19,20] and the validity of the quasiparticle picture. In Sec. III B we calculate in addition the ground-state energies in the high-doping regime and comment on hole pairing and the possibility of hole clustering or phase separation.[21–26] Apart from being relevant to the theory of high-T_c superconductivity, the Hubbard-like models also provide insight into other fascinating problems like magnetic phenomena[27,28] and transport or metal insulator transitions.[29,30] The stability of the ferromagnetic state in the $U = \infty$ Hubbard model especially has been studied intensively and controversially.[31–34] In Sec. III C we will discuss the question by exactly diagonalizing an 18-site cluster with an arbitrary number of holes. Finally, in Sec. IV we summarize our results.

II. MODEL AND METHOLOGY

A. Strong-coupling Hamiltonian

The starting point of our work is the two-dimensional one-band Hubbard model defined by the Hamiltonian

$$H=-t\sum_{\langle ij\rangle,\sigma}(c_{i\sigma}^{\dagger}c_{j\sigma}+\text{H.c.})+\frac{U}{2}\sum_{i,\sigma}n_{i\sigma}n_{i-\sigma}\ . \quad (1)$$

Here the operators $c_{i\sigma}^{\dagger}(c_{i\sigma})$ create (destroy) a spin σ electron in a Wannier state at site i and $n_{i\sigma}=c_{i\sigma}^{\dagger}c_{i\sigma}$. The first term represents the kinetic energy of electrons on a square lattice, where the transfer amplitudes t are restricted to nearest-neighbor $\langle ij\rangle$ hopping processes. In the strong-coupling limit of large Coulomb interaction ($U\gg t$) it appears to be sensible to describe the low-energy excitations of the Hubbard model within the subspace of minimal number of doubly occupied sites. Using the particle-hole symmetry and restricting ourselves to the case of electron density $n\leq 1$, one can derive the strong-coupling Hamiltonian using a canonical transformation[6,7,35] up to order t^2/U:

$$H_{\mathrm{SC}}=H_1+H_2+H_3\ , \quad (2)$$

$$H_1=-t\sum_{\langle ij\rangle,\sigma}(\tilde{c}_{i\sigma}^{\dagger}\tilde{c}_{j\sigma}+\text{H.c.})\ , \quad (3)$$

$$H_2=\frac{4t^2}{U}\sum_{\langle ij\rangle}\left[\mathbf{S}_i\mathbf{S}_j-\frac{n_in_j}{4}\right]\ , \quad (4)$$

$$H_3=-\frac{t^2}{U}\sum_{\langle ijk\rangle,\sigma}[(\tilde{c}_{i\sigma}^{\dagger}\tilde{c}_{j-\sigma}^{\dagger}\tilde{c}_{j-\sigma}\tilde{c}_{k\sigma}+\tilde{c}_{i-\sigma}^{\dagger}\tilde{c}_{j-\sigma}\tilde{c}_{j\sigma}^{\dagger}\tilde{c}_{k\sigma})+\text{H.c.}]\ , \quad (5)$$

with $\mathbf{S}_i=\frac{1}{2}\sum_{\alpha,\beta}\tilde{c}_{i\alpha}^{\dagger}\boldsymbol{\sigma}_{\alpha\beta}\tilde{c}_{i\beta}$, $n_i=n_{i_\uparrow}+n_{i_\downarrow}$, and $n_{i\sigma}=\tilde{c}_{i\sigma}^{\dagger}\tilde{c}_{i\sigma}$.

The operators $\tilde{c}_{i\sigma}=c_{i\sigma}(1-n_{i-\sigma})$ are chosen to constrain the configurations to those without double occupancy, thereby reducing the dimension of the Hilbert space from 4^N to 3^N, where N is the number of sites. Note that the first term is now connected to the motion of $(1-n)N$ holes in the lower Hubbard band, hence its energy tends to zero if $n\rightarrow 1$. H_1 and H_2 constitute the t-J model with the antiferromagnetic Heisenberg exchange interaction $J=4t^2/U$, which is generated through a virtual double occupancy during a two-site hopping process.[36] H_3 describes virtual three-site hopping processes where $\langle ij\rangle$ and $\langle jk\rangle$ are nearest neighbors. This contribution is of the order of t/U smaller than the leading hopping term, but it should be emphasized that the first term of H_3 just describes sublattice hopping of a hole and therefore leaves, e.g., the Néel spin background unchanged.[37] The full Hamiltonian H_{SC} defines the t-t'-J model[9,10] with $t'=t^2/U$, which should not be confused with models where t' denotes a direct intrasublattice transfer.[16,38]

Obviously, with respect to its applicability to high-temperature superconductivity the $\mathrm{Cu}_{3d_{x^2-y^2}}-O_{2p_{x,y}}$ model proposed by Emery[39] should be a more realistic starting point. Due to the Zhang-Rice argument,[40] however, it is assumed that the low-energy spectrum of this model can in the relevant parameter regime be mapped quite accurately onto an effective one-band model of hopping and exchange;[38] for a further discussion of this point see Ref. 41. Irrespective of the fact that the t-J or better the t-t'-J model describes the behaviors of the Emery[39] and the one-band Hubbard model only for $t/U\ll 1$, the t-J model can be studied as a model of its own right in the whole parameter regime[42] of t and J even in the limit $J\gg t$.

Unfortunately there are very few exact analytical results for the infinite two-dimensional Hubbard or t-J system. While it is generally accepted that the ground state on a square lattice with one electron per site shows antiferromagnetic order, the situation upon doping[43] is much less clear except in the Nagaoka limit.[44,45] To obtain more insight into these systems a number of numerical studies has been performed,[9–16,46,47] where most of the exact diagonalizations are done for the "simpler" t-J model with 16 sites.

B. Numerical technique

We consider tilted $\sqrt{18}\times\sqrt{18}$ and $\sqrt{20}\times\sqrt{20}$ clusters with periodic boundary conditions which cover the whole square lattice. The case of antiperiodic and mixed boundary conditions was recently examined by Riera[48] with respect to two-hole binding energies on smaller clusters and the results are qualitatively insensitive to the boundary conditions used.

Previous numerical investigations on the 4×4 cluster gave rise to controversial interpretations due to the high symmetry of this cluster, which is larger than the point group C_{4v} of the square lattice, causing an accidental degeneracy of the ground state.[11–13] This is very unfortunate if one wants to answer the question regarding the position of the hole pockets, because the only considered candidates[19,20] for this position are $(\pm\pi/2,\pm\pi/2)$, and $(\pm\pi,0)$, and $(0,\pm\pi)$, which are energetically degenerate on the 4×4 lattice. The $\sqrt{18}\times\sqrt{18}$ and the $\sqrt{20}\times\sqrt{20}$ lattices do not possess this additional symmetry; the allowed $\mathbf{K}$ vectors are depicted in Fig. 1 for both lattice sizes. Besides using translational invariance to reduce the dimension of the Hilbert space we can exploit the point group symmetries contained in the little group of $\mathbf{K}$. Finally, the Hamiltonian H_{SC} is spin rotational invariant, so we can as usual work in the subspace of fixed total S^z. The maximum dimensions of the unsymmetrized (symmetrized) Hilbert space we considered were 9 237 800 (461 890) [$N=20$, $N_h=2$, any $\mathbf{K}$, $S^z=0$] and 17 153 136 (953 088) [$N=18$, $N_h=6$, $\mathbf{K}=(0,0)$, $S^z=0$] (only translations). Note that most of the nonvanishing matrix elements of H_{SC} arise from the H_3 term; for example, for $N=20$, $N_h=2$, $S^z=0$, H_3 produces 9 677 904 of the 21 516 834 nonzero matrix elements.

In order to calculate the eigenvalue spectrum we used a Lanczos method which is different from the one proposed by Dagotto and Moreo.[49] In their method the Hamiltonian is projected onto Krylow subspaces of dimension m parametrized by a starting vector ψ_0 much smaller than the dimension of the Hilbert space. One then diagonalizes the resulting tridiagonal matrix T^m—the Lanczos matrix—and uses the back-transformed

eigenvector corresponding to the lowest eigenvalue of T^m as a starting vector ψ_0' for the next subspace generation. Iterating this procedure the starting vector will converge to the ground-state eigenvector and the lowest eigenvalue of T^m converges to the ground-state energy. In our Lanczos method we follow more closely the algorithm described by Cullum and Willoughby.[50] Starting with any vector that is *not* an eigenvector, we generate the Lanczos matrices T^m. Increasing m we check for the convergence of an eigenvalue of T^m in a specified range. In this way we can avoid spurious eigenvalues for fixed Lanczos dimension m, which disappear[50] as one varies m. Sturm sequencing is used to effectively calculate the desired eigenvalue of T^m and allows for using results of tridiagonalization for smaller values of m. Since this method directly iterates for the eigenvalue it is generally faster than a method that iterates for an eigenvector. Sturm sequencing also allows to generate more eigenvalues than just the ground state, which is necessary if one wants to classify eigenvalues according to S. Our numerical procedure was checked,[47] by reproducing the lowest eigenvalue for the pure t-J model obtained in Refs. 13 and 16 ($N=16,18$; $N_h=1,2$); whereas for the case $N=18$, $N_h=1$ we found lower eigenvalues than those stated by Elser *et al.*[15] at several **K** points.

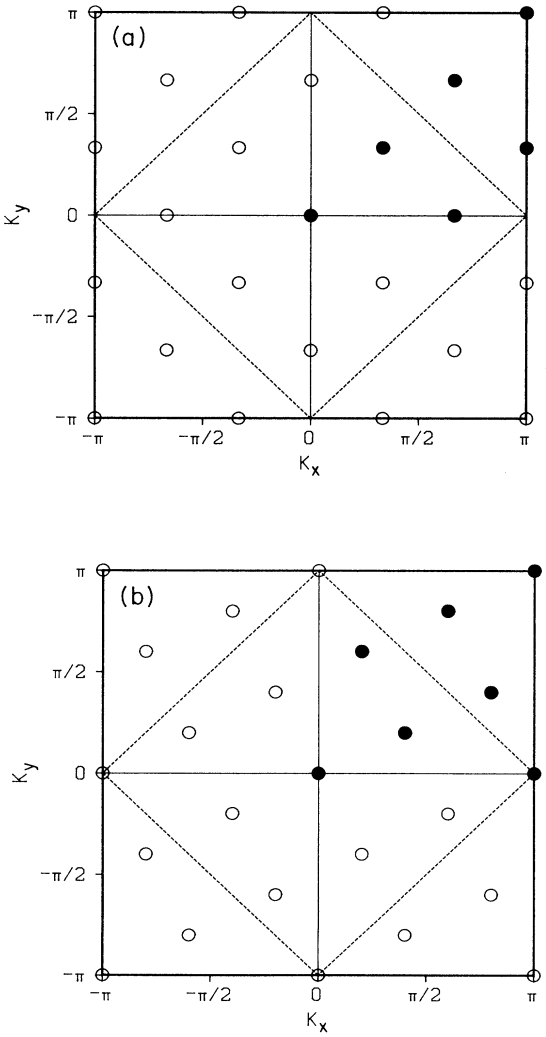

FIG. 1. Brillouin zone of the (a) 18-site and (b) 20-site lattice with periodic boundary conditions. Solid circles represent the **K** vectors unrelated by symmetry; the dashed square defines the pseudo Fermi surface at half filling.

III. RESULTS OF THE FINITE-LATTICE STUDY

A. Single-hole properties

Here we shall discuss the results for the one-hole sector. The momentum **K**, total spin S, and the symmetry classification of the ground state are given in Table I for both the t-J and the t-t'-J model as a function of U on the 18- and 20-site lattices (here and in the following all energies are measured in units of t). As mentioned above the ground state is nondegenerate and as the Coulomb energy increases its momentum is shifted from a value near the perfect nested Fermi surface of the half-filled Hubbard model to (0,0) $[(\pi,\pi)]$ for $N/2$ odd [even] near the Nagaoka transition.[44] At this value of U the ground state becomes fully ferromagnetically polarized ($S=S_{\max}$ for $U \geq U_c$). The nonmonotonic behavior of the momentum of the Nagaoka state is caused by the finiteness of the system in connection with periodic boundary conditions; the same change of momentum can be seen in the ($N_h=0$) Heisenberg ground state. As illustrated in Fig. 2 this behavior is smeared out for larger lattice sizes. The difference of ground-state energies $E[\mathbf{K}=(0,0)] - E[\mathbf{K}=(\pi,\pi)]$ tends—as it should—to zero in the limit $N \to \infty$ (alternating in sign).

To address the question whether there are hole pockets in the Fermi surface of the infinite system (if such a Fermi surface exists) we discuss the energy dispersion $E(\mathbf{K},S)$ of the vacancy band. Our calculations were always done in a subspace of fixed total S^z, which only imposes a lower bound on the total spin S. Since, depending on **K**, S-level crossings occur even at relative small values of U ($U=10$), we have to determine those excited states of a lower S^z sector which are not contained in the higher S^z sectors to obtain a band dispersion with definite S. For $N=18$ (20) we have six (seven) inequivalent wave vectors $\mathbf{K}_i$ (cf. Fig. 1) in the Brillouin zone. We can extend these six (seven) energies $E(\mathbf{K}_i,S;\ N_h=1)$ throughout the whole Brillouin zone by the following energy dispersion:

$$E(\mathbf{K},S)=\sum_{\substack{l,m=0 \\ (l+m)\leq 3}} a_{lm} \cos lK_x \cos mK_y \ . \tag{6}$$

We want to emphasize that such a band classification due to S was carried out for the first time in Ref. 47 for

TABLE I. The classification of the one-hole ground state on a 18- and 20-site lattice due to momentum **K**, total spin S, and irreducible representation (IR) of the point group $G(\mathbf{K})$ involved, at various interaction strengths U.

N	**K**	S	IR	$G(\mathbf{K})$	t-J	t-t'-J
18	$\left(\frac{2\pi}{3},0\right)$	$\frac{1}{2}$	A'	C_s	$U\leq 21.5$	$U\leq 27.7$
	$\left(\frac{\pi}{3},\frac{\pi}{3}\right)$	$\frac{1}{2}$	A'	C_s	$21.6\leq U\leq 77.3$	$27.8\leq U\leq 85.7$
	(0,0)	$\frac{1}{2}$	A_1	C_{4v}	$77.4\leq U\leq 84.6$	$85.8\leq U\leq 91.5$
	(0,0)	$\frac{17}{2}$	A_1	C_{4v}	$U\geq U_c=84.7$	$U\geq U_c=91.6$
20	$\left(\frac{\pi}{5},\frac{3\pi}{5}\right)$	$\frac{1}{2}$	A	C_1	$U\leq 72.6$	$U\leq 78.7$
	$\left(\frac{2\pi}{5},\frac{\pi}{5}\right)$	$\frac{1}{2}$	A	C_1	$72.7\leq U\leq 74.5$	$78.8\leq U\leq 83.8$
	(0,0)	$\frac{1}{2}$	B	C_4	$74.6\leq U\leq 96.6$	$83.9\leq U\leq 103.4$
	(π,π)	$\frac{19}{2}$	B	C_4	$U\geq U_c=96.7$	$U\geq U_c=103.5$

$N=18$. Figures 3(a) and 3(b) show as a comparison the results for $N=20$ for both the t-J and t-t'-J models for $U=10$. First we notice that, for not too small exchange interactions $J/t>0.2$, the minima of the lowest $S=\frac{1}{2}$ band are well separated from bands belonging to higher spin sectors, while around $\mathbf{K}=(0,0)$, (π,π) higher spin sectors become lower in energy. So for this parameter range we conclude from our finite-size data that a usual spin-$\frac{1}{2}$ quasiparticle description may be adequate. Increasing the Coulomb interaction strength ($U>40$) the states with larger spin become comparable in energy, a situation which suggests the formation of ferromagnetic polarons.[51] Defining as Elser *et al.*[15] a coherent bandwidth

$$\Delta E=\sup[E(\mathbf{K},S)]-\inf[E(\mathbf{K},S)]\ , \tag{7}$$

we observe that ΔE becomes very small at $U=U_c$ ($\Delta E=0.027$ for $N=20$) and tends to zero in the thermodynamic limit. As pointed out many times,[4,10,20] due to coupling of spin and hole dynamics the characteristic energy for the hole motion is J and not t in the limit $t>J$.

In this work no attempt is made to discuss the hole spectral function

$$A_{\mathbf{K}\sigma}(\omega)=\sum_m |\langle\psi_m^{N-1}|c_{\mathbf{K}\sigma}|\psi_0^N\rangle|^2\delta(\omega+E_m^{N-1}-E_0^N)\ , \tag{8}$$

calculating the overlap between the state where one hole is created in the Heisenberg ground state $|\psi_0^N\rangle$ and the exact eigenstates of the one-hole subspace (see Refs. 52–54). While for $J=0$ the spectrum is completely incoherent, for finite J it shows a well-separated quasiparticle peak of width $\sim J$ below a broad incoherent spectrum. The energy dispersion, which can be derived from this dominant peak,[37,54–56] can be related directly to our $S=\frac{1}{2}$ band, thereby yielding additional evidence for the validity of the suggested quasiparticle description in this parameter regime.

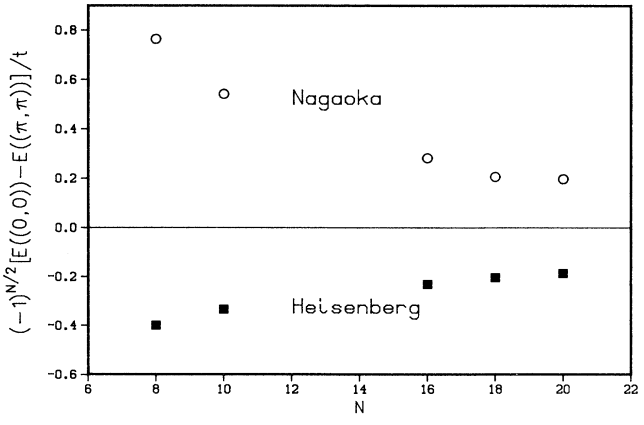

FIG. 2. The energy difference $(-1)^{N/2}\,[E(0,0)-E(\pi,\pi)]$ is given for increasing lattice size N, where $E(\mathbf{K})=\min_S E(\mathbf{K},S)$. The open circles show the Nagaoka limit: $N_h=1$, $U=\infty$; the solid squares the Heisenberg limit: $N_h=0$ at $U=10$.

Poilblanc and Dagotto[20] suggested that the hole momenta of minimal energy might depend on the inclusion of terms like H_3 in Eq. (2). Indeed, our numerical results for the full Hamiltonian H_{SC} lead to a minimum of $E(\mathbf{K},\frac{1}{2})$, which is located on the *corners* of the pseudo-Fermi surface, whereas the pure t-J model gives the minima at $(\pm\pi/2,\pm\pi/2)$. This is impressively demonstrated through the contour plots in Figs. 4–7 which show the energy dispersion [Eq. (6)] in the $S=\frac{1}{2}$ sector for both models and various U values extended over the whole Brillouin zone. Notice that the 18- and 20-site clusters lead to qualitatively the same results. In contrast to the noninteracting case (where doped holes distribute themselves uniformly along the Fermi surface indicated through the dashed line in Fig. 1), the holes in the interacting case will upon doping accumulate near the minima of the band dispersion [Eq. (6)] (indicated by large dots in Figs. 4–7), and form a pocketlike Fermi surface. These hole pockets are most pronounced for $U=4$ and weaken with increasing U. At the same time the position of the minima moves away from the magnetic Brillouin-zone boundary, while the whole band structure flattens out. The difference in position of the pockets of the t-J and t-t'-J models disappears for U greater than about 20 when the influence of the H_3 term ($\sim 1/U$) is weakened. Since the t-t'-J model is a better approximation to the Hubbard model, it is interesting to speculate whether the Hubbard model also forms hole pockets around $(\pm\pi,0)$, $(0,\pm\pi)$. In order to answer this question one would have to study the Hubbard model on at least a 18-site lattice because of the accidental degeneracy of the 16-site lattice mentioned above. Quantum Monte Carlo calculations[17] do not find evidence for hole pockets in the Hubbard model, but these simulations cannot be performed at those low temperatures, which are necessary to resolve the small energy differences ($\sim 0.1t$ for $U=10$, $N=18$) along the pseudo-Fermi surface.

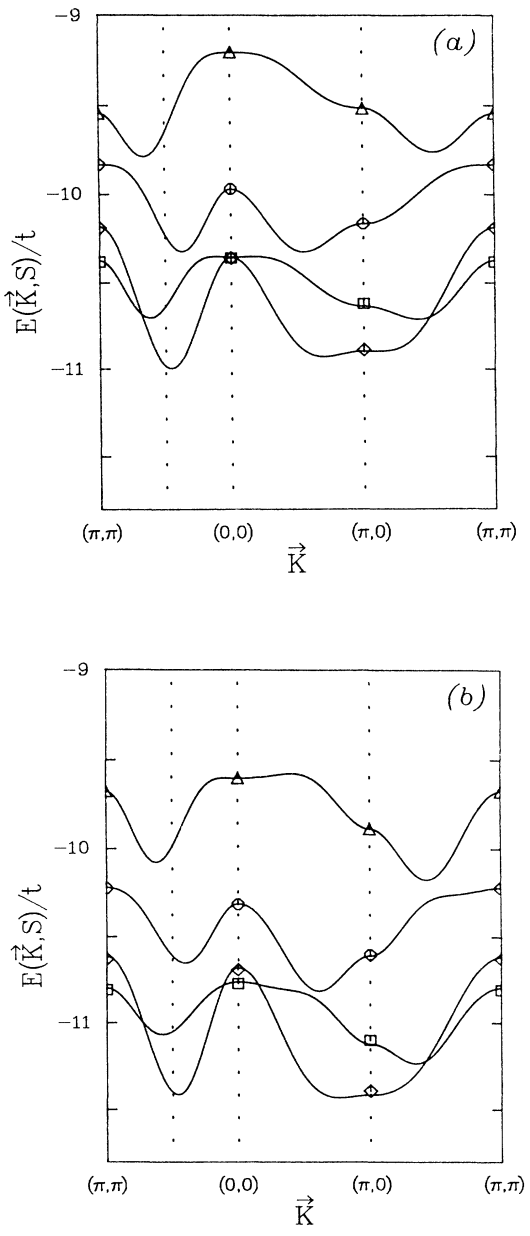

FIG. 3. Band structure for a single hole on the 20-site lattice. The symbols denote different total spins [S: $\frac{1}{2}$ (◇); $\frac{3}{2}$ (□); $\frac{5}{2}$ (○); and $\frac{7}{2}$ (▽)] at the allowed $\mathbf{K}$ values. The interpolation is done with Eq. (6) for the (a) t-J and (b) t-t'-J models at $U=10$.

As pointed out by Schrieffer, Wen, and Zhang[19] the formation of a pocketlike Fermi surface is important to give a nodeless pairing gap over the whole Fermi surface (as most experiments indicate), although its formal symmetry can be of p- or d-wave type. Another interesting difference between the t-J and the t-t'-J models appears if one calculates the components of the effective-mass tensor parallel and perpendicular to $\mathbf{K}_{min}$ at $\mathbf{K}_{min}$. Apart from the well-known increase in effective band mass with increasing U (cf. Ref. 57), the effective mass tensor for $U \lesssim 20$ is rather isotropic for the t-t'-J model and strongly anisotropic for the t-J model (see Table II).

B. Pairing and phase separation

In Table III we present the values for the ground-state energy with respect to the Heisenberg energy $\bar{E}(N_h)=E(N_h)-E(0)$ and the complete symmetry classification of the ground state for up to four (two) holes for both the t-J and t-t'-J model on the 18- (20-) site lattice for $U=10$. It is known from a series of Lanczos studies[11–13] for smaller lattices that the ground state for two holes is found to be a spin singlet ($S=0$) independent of U. For our larger systems, however, the $\mathbf{K}$ degeneracy of the ground state is lifted. The $\mathbf{K}$ dependence of the two-hole ground state is shown in Fig. 8 for the singlet ($S=0$) and the triplet ($S=1$) cases. The $S=0$ state exhibits at $\mathbf{K}=(0,0)$ a well-defined minimum and, as in the case of one hole, its total energy is reduced due to the inclusion of the H_3 term.

Of special interest is the question whether there is hole binding or clustering. To comment on this problem we have computed the binding energies of various numbers of holes defined by

$$
\begin{aligned}
E_B^2 &= E(2)+E(0)-2E(1)\,, \\
E_B^3 &= E(3)+E(0)-E(2)-E(1)\,, \\
E_B^4 &= E(4)+E(0)-2E(2)\,, \\
E_B^6 &= E(6)+E(0)-E(4)-E(2)\,,
\end{aligned}
\tag{9}
$$

where we chose those decompositions that maximize $E_B^{N_h}$ and therefore give the highest probability for the specific "dissociation channel." The various binding energies for the pure t-J model for the 16- and 18-site lattice are presented in Figs. 9(a) and 9(b) as a function of J. As mentioned previously[12,58] there exists a parameter range ($10 \le U \le 40$) within which E_B^2 is negative but $E_B^{N_h}$ ($N_h > 2$) are positive. This gives evidence for hole pairing but not for hole clustering. It should be stressed that the binding energy for two holes for the 18- and 20-site clusters in this parameter regime is more negative than the

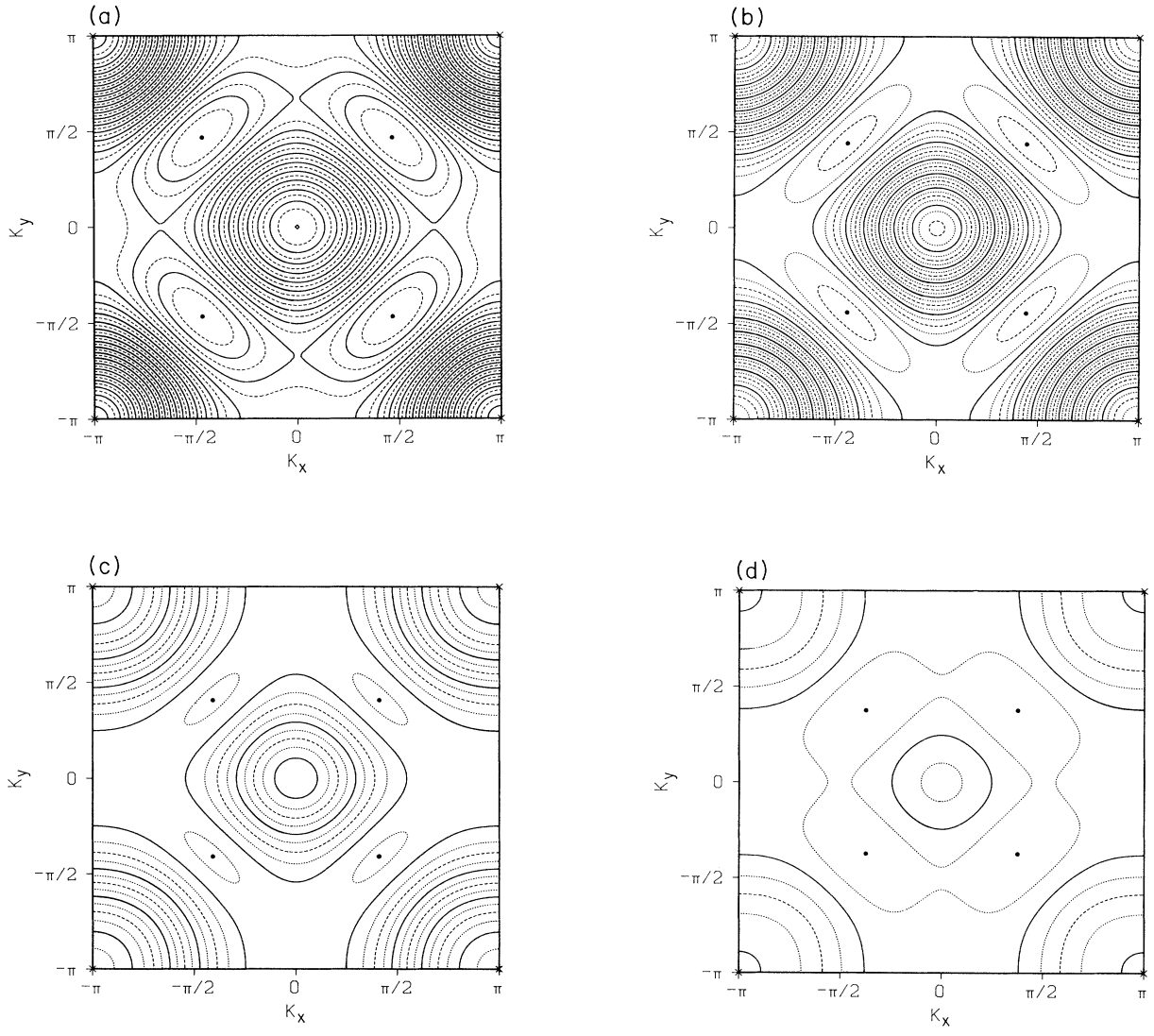

FIG. 4. Contourplots of the "quasihole" energy dispersion $E(\mathbf{K}, \frac{1}{2})$ in the Brillouin zone of the square lattice. The lines of constant energy are derived from the t-J model on the $\sqrt{18}\times\sqrt{18}$ lattice at various Coulomb repulsions (a) $U=4$, (b) 10, (c) 20, and (d) 40. The crosses mark the maximum of $E(\mathbf{K}, \frac{1}{2})$ at the corners of the Brillouin zone, whereas the closed circles denote the minimum (cf. Fig. 3). The energy difference between neighboring solid lines is $0.1t$.

one for the smaller 16-site system. The same is true for the t-t'-J model.[47] Whether these results allow for the conclusion that there is pairing in the infinite system still remains controversial. Note that this binding is weakened and finally lifted if we include longer range Coulomb forces like

$$H_4 = \sum_{i,j} V_{ij} n_i n_j \tag{10}$$

into our Hamiltonian (cf. Refs. 26 and 47). In a more realistic two-band model H_4 reflects the Coulomb repulsion between charged singlets.[4] Figure 9 indicates that the parameter range within which the finite-size results may be consistent with hole clusters ($J > t$) are outside the regime of validity of the strong-coupling expansion. Therefore we did not use the H_3 term for these studies.

Recently Emery, Kivelson, and Lin[22] suggested that the t-J model shows an instability towards phase separation at all J, which means that upon doping the system would separate into a hole-rich phase and an antiferromagnetic phase without holes. In order to obtain the energy of such a two-phase state it is necessary to minimize the total energy of a system with N_s sites,

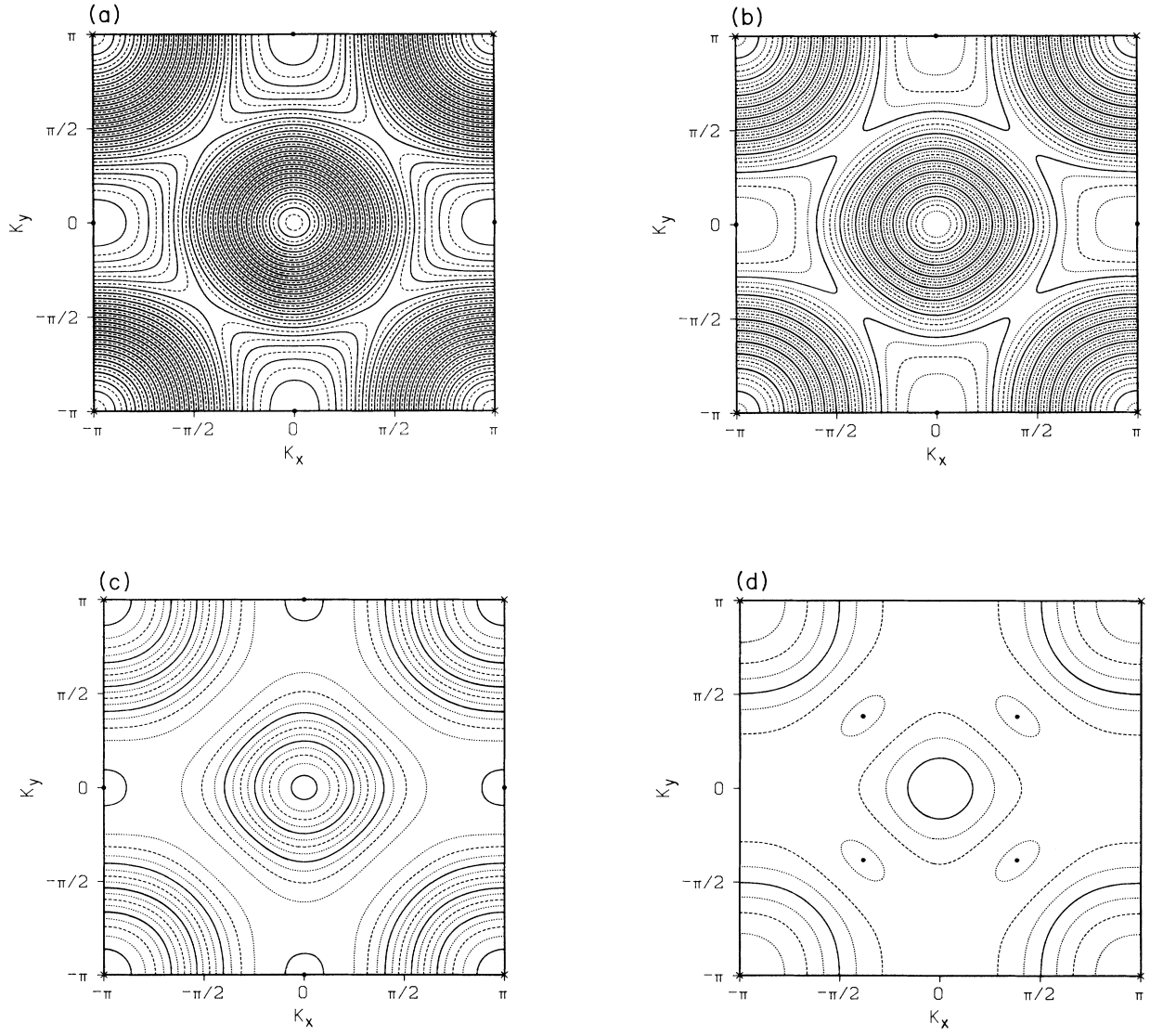

FIG. 5. Contourplots of $E(\mathbf{K}, \frac{1}{2})$ derived from the t-t'-J model on a 18-site lattice. The parameters are the same as in Fig. 4.

$E=(N_s-N)e(0)+Ne_h(x)$, with respect to the portions (N_s-N) and N of the antiferromagnetic and the hole-rich phase. The energy per site of the hole-rich phase $e_h(x)$ depends only on the concentration $x=N_h/N$ of holes. Phase separation then exists for concentrations $x<x_m$ provided the function $e(x)=[e_h(x)-e(0)]/x$ exhibits a minimum[22] at $x=x_m$. Here the free energy becomes a concave function[24] of x. The function $e(x)$ was computed from a finite-size calculation with 16 sites by Emery, Kivelson, and Lin.[22] The crucial step in such a calculation is that the energy of a finite cluster with N_h holes is interpreted as the energy of the hole-rich phase with hole concentration $x=1-n$. The function $e(x)$ is shown in Fig. 10 for the t-J model for various values of the exchange coupling. Obviously we must distinguish between two regimes of the exchange coupling. In the strong-coupling regime $J\ll t$ the minimum of $e(x)$ is shifted to lower concentrations raising the system size from 10,16,18 to 20 sites (cf. Refs. 26 and 47) for $U=10,20$. This is due to the fact that the minimum is always connected to the two-hole ground state (provided $E_B^2<0$, i.e., $U\lesssim 50$). Our finite-size results do not allow for the identification of x_m by Emery, Kivelson, and Lin[22] as a critical concentration for the occurrence of phase separation in this parameter range. For larger values of J we find different behavior. Here the minimum is more pronounced and is shifted towards $x=1$ for $J\gg t$, which means towards the fully phase-separated state where the hole-rich phase contains no electrons. The possibility of hole clustering in this parameter regime is also visible in

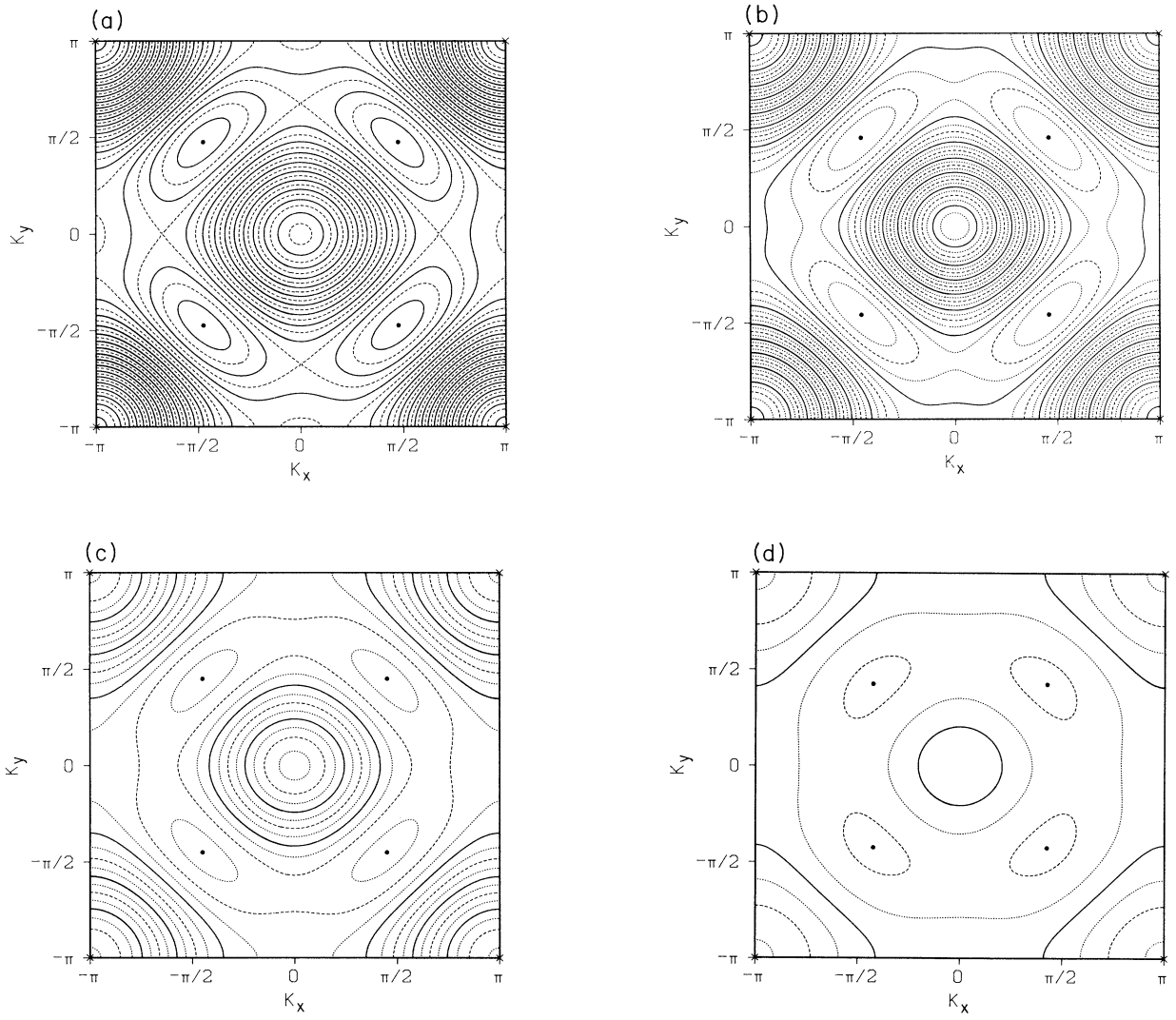

FIG. 6. Contourplots of the band dispersion $E(\mathbf{K},\frac{1}{2})$ as in Fig. 4, but now constructed from the results for the t-J model on 20-site lattice.

Fig. 9. If one calculates the inverse isothermal compressibility per site[59]

$$\kappa^{-1}=n^2\left[\frac{E(N_e+2)+E(N_e-2)-2E(N_e)}{4N}\right], \quad (11)$$

we notice that κ^{-1} becomes negative for $x<x_m$, rendering the system unstable [in finite-size systems it is favorable to compare quantities with even (odd) numbers of holes separately; see Fig. 10]. We would like to state two additional remarks on the question of phase separation. First, the minimum of $e(x)$ is destroyed quite rapidly by the inclusion of even a moderate interatomic Coulomb repulsion as shown in Ref. 26, thereby restoring the homogeneity of the system. Second, calculations of the thermodynamic quantities of finite systems have shown that particle number fluctuations in a grand canonical treatment also destroy phase separation,[60] for not too large J/t.

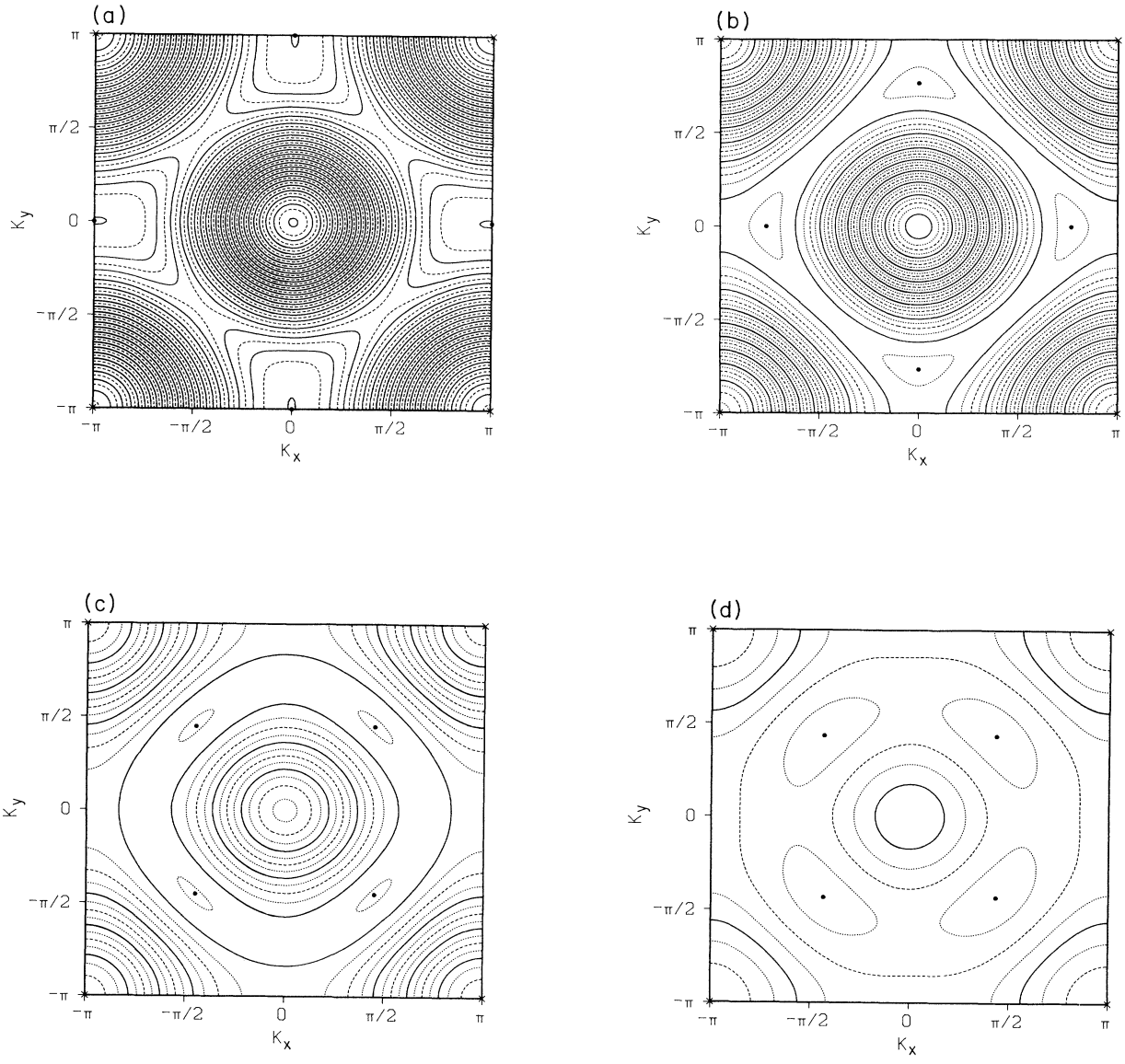

FIG. 7. Band structure of the t-t'-J model on a 20-site lattice from Eq. (6) with the same parameters as in Fig. 6.

TABLE II. Components of the effective-mass tensor at the minimum of the band dispersion $E(\mathbf{K},\frac{1}{2})$ (for the $\sqrt{18}\times\sqrt{18}$ lattice) located at $\mathbf{K}_{\min}$. $(m^*/m)_\parallel$ and $(m^*/m)_\perp$ denote the values parallel and perpendicular to $\mathbf{K}_{\min}$, respectively.

	U	$\mathbf{K}_{\min}$	$\left[\left(\frac{m^*}{m}\right)_\parallel;\left(\frac{m^*}{m}\right)_\perp\right]$
t-J	4	$0.94\left(\frac{\pi}{2},\frac{\pi}{2}\right)$	(0.69; 3.54)
	10	$0.89\left(\frac{\pi}{2},\frac{\pi}{2}\right)$	(1.30; 15.67)
	20	$0.82\left(\frac{\pi}{2},\frac{\pi}{2}\right)$	(2.81; 31.55)
	40	$0.75\left(\frac{\pi}{2},\frac{\pi}{2}\right)$	(7.01; 20.46)
t-t'-J	4	$(\pi,0)$	(2.72; 1.60)
	10	$(\pi,0)$	(9.87; 5.55)
	20	$(\pi,0)$	(22.82; 19.72)
	40	$0.77\left(\frac{\pi}{2},\frac{\pi}{2}\right)$	(6.02; 24.29)

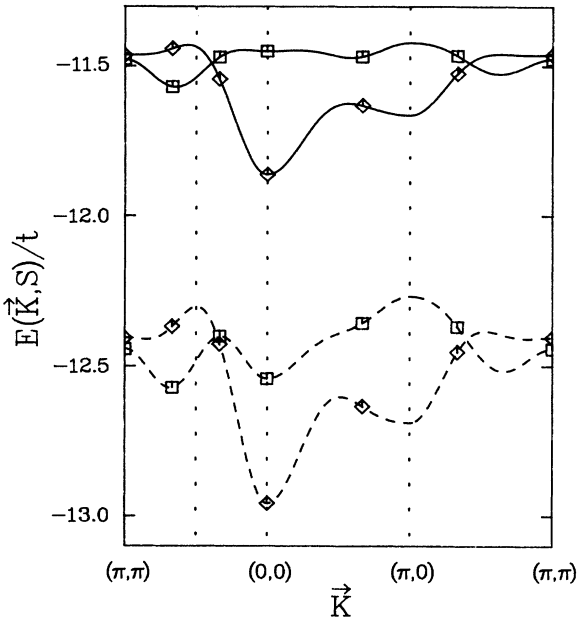

FIG. 8. **K**-dependence of the ground state energy of two holes in the $S=0$ (◇) and $S=1$ (□) spin sector. The solid (dashed) lines are calculated for the t-J (t-t'-J) model on a $\sqrt{18}\times\sqrt{18}$ lattice at $U=10$.

C. The limit $U=\infty$

In this section we give a complete description of exact results for the ground state of the Hubbard model on the 18-site lattice in the infinite-U limit. The probability for the appearance of ferromagnetic states is largest for $U=\infty$, since for finite U there is always an effective antiferromagnetic exchange interaction. In the infinite-U limit the Hubbard-Hamiltonian reduces to H_1. At half-filling, due to the two possible spin orientations per site, there exists a large 2^N-fold ground-state degeneracy. In the one-hole case one has the exact result of Nagaoka[44] stating that the ground state on a bipartite lattice has

TABLE III. Energy $\bar{E}$, spin, momentum, and symmetry group of the ground state for up to four (two) holes on a $\sqrt{18}\times\sqrt{18}$ ($\sqrt{20}\times\sqrt{20}$) lattice at $U=10$.

N	N_h	$\mathbf{K}$	S	IR	$G(\mathbf{K})$	$\bar{E}(N_h)$ t-J	t-t'-J
18	1	$\left(\frac{2\pi}{3},0\right)$	$\frac{1}{2}$	A'	C_s	−1.415 274	−1.938 938
	2	(0,0)	0	A_1	C_{4v}	−3.266 077	−4.360 609
	3	$\left(\frac{2\pi}{3},0\right)$	$\frac{1}{2}$	A'	C_s	−4.713 952	−6.167 221
	4	(0,0)	0	A_1	C_{4v}	−6.372 600	−8.094 627
20	1	$\left(\frac{\pi}{5},\frac{3\pi}{5}\right)$	$\frac{1}{2}$	A	C_1	−1.440 691	−1.930 823
	2	(0,0)	0	A	C_4	−3.273 336	−4.288 678

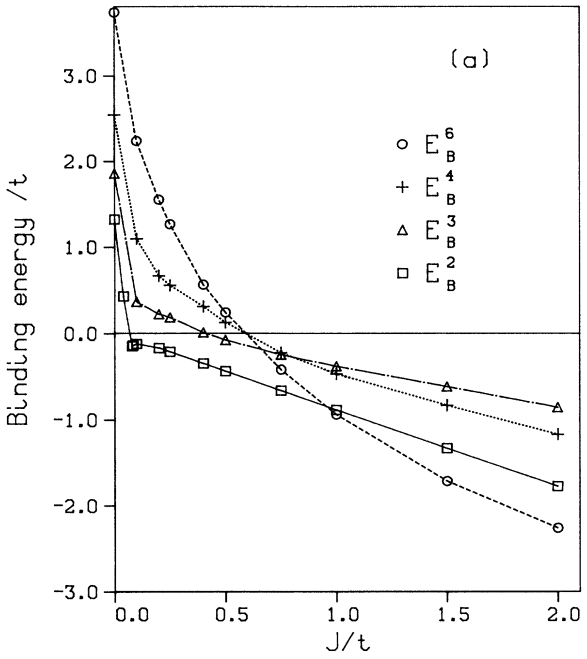

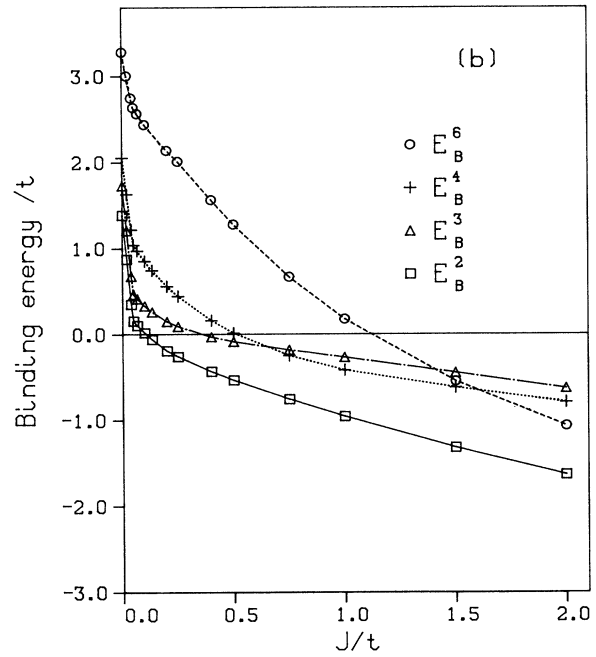

FIG. 9. Binding energies $E_B^{N_h}$ for $N_h=2$ (□), 3 (△), 4 (+), and 6 (○) holes added to the half-filled band are depicted for the t-J model vs exchange energy J in (a) and (b) for the 4×4 and $\sqrt{18}\times\sqrt{18}$ lattices, respectively.

maximal total spin. For any finite number of holes in the infinite lattice—that means $x=0$—it is argued[45] that the ground state is degenerate with the ferromagnet $S=S_{\max}$ and the ground-state energy is given by $E(N_h, N=\infty, U=\infty)=-4N_h t$. No further rigorous results are available, so it seems a fascinating task to determine the spin structure which minimizes the kinetic energy of holes. In the limit of small electron densities n there should be a paramagnetic ground state following the old Kanamori argument.[61] In the opposite limit $x \ll 1$ investigations of the stability of the *saturated* ferromagnetic state with respect to single spin flips using variational wave functions show its instability at hole density $x=0.49$ (cf. Ref. 33). A diagonalization study on the 16-site lattice by Riera and Young[14] leads to a highly nonmonotonic behavior of total spin S as the number of holes increases.

Our results for the 18-site cluster are reported in Table IV. Again one observes nonmonotonic behavior of S as a function of hole density which renders an extrapolation to the thermodynamic limit difficult. Near quarter-filling, however, there is a region with large S. The state with nine holes exhibits as the Nagaoka state *maximal* total spin; the nine electrons can therefore be described as spinless fermions which occupy the nine allowed **K** values within the magnetic Brillouin zone [cf. Fig. 1(a)]. Spin multiplets are obviously connected to "less symmetric" irreducible representations of the point group

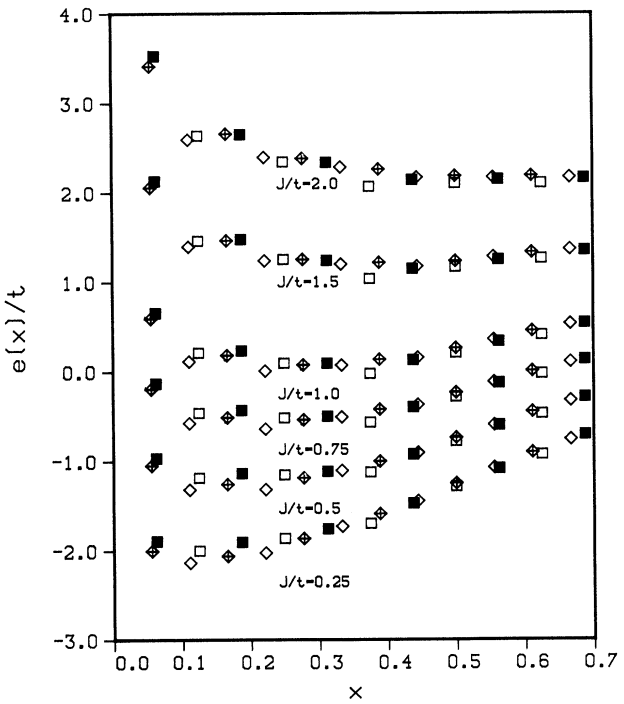

FIG. 10. The function $e(x)$ (see text) is shown as a function of hole concentrations x for different exchange energies J. The (tilted) squares belong to the lattice with (18) 16 sites, where open symbols correspond to even numbers of holes N_h.

TABLE IV. Energy and symmetry classification of the ground state, as a function of hole number, for the $U=\infty$ model on the $\sqrt{18}\times\sqrt{18}$ lattice with periodic boundary conditions.

N_h	K	S	IR	$G(\mathbf{K})$	E
1	(0,0)	$\frac{17}{2}$	A_1	C_{4v}	−4.000 000
2	(0,0)	0	A_1	C_{4v}	−6.613 382
3	$\left(\frac{\pi}{3},\frac{\pi}{3}\right)$	$\frac{1}{2}$	A'	C_s	−8.885 234
4	(0,0)	0	A_1	C_{4v}	−11.174 222
5	$\left(\frac{2\pi}{3},0\right)$	$\frac{3}{2}$	A''	C_s	−13.082 963
6	(π,π)	1	B_1	C_{4v}	−14.507 345
7	(0,0)	$\frac{5}{2}$	B_1	C_{4v}	−15.400 480
8	(0,0)	4	A_2	C_{4v}	−16.196 909
9	(0,0)	$\frac{9}{2}$	A_2	C_{4v}	−16.000 000
10	(0,0)	0	B_2	C_{4v}	−15.594 873
11	$\left(\frac{\pi}{3},\frac{\pi}{3}\right)$	$\frac{3}{2}$	A''	C_s	−14.898 537
12	(0,0)	2	B_1	C_{4v}	−14.227 499
13	$\left(\frac{\pi}{3},\frac{\pi}{3}\right)$	$\frac{3}{2}$	A''	C_s	−12.627 526
14	(0,0)	0	B_2	C_{4v}	−11.040 411
15	$\left(\frac{\pi}{3},\frac{\pi}{3}\right)$	$\frac{1}{2}$	A'	C_s	−9.312 771
16	(0,0)	0	A_1	C_{4v}	−7.621 233
17	(0,0)	$\frac{1}{2}$	A_1	C_{4v}	−4.000 000

$G(\mathbf{K})$. Let us stress that Barbieri, Riera, and Young[31] have recently pointed out that the instability of the Nagaoka state for small numbers of holes N_h is an artifact of the small cluster size. They showed that the ferromagnetic state is in general locally stable with respect to single-spin flips for $N_h \ll \ln N$. Our results do obviously not prove the existence of a ferromagnet for finite hole densities. We believe, however, that they show at low doping level $x<0.5$ a tendency of the system to form a ground state which is not a singlet. The same is argued by Zhou and Gong[34] from a different point of view. They showed that ferromagnetic correlations affect the motion of more than one hole through forming flux phases, where the total spin remains almost the same as that of the satured ferromagnet.

IV. CONCLUSIONS

In this paper we have reported results on finite clusters with varying numbers of holes. A modified Lanczos algorithm allowed us to classify ground states according to their total spin S and therefore to investigate the effective band structure.

In the one-hole sector we found the quasiparticle picture to be appropriate for not too large values of U. A comparison of the t-J and t-t'-J models showed qualitative differences in this parameter range: the position of the hole pockets is shifted from $(\pm\pi/2,\pm\pi/2)$ for the t-J model to $(\pm\pi,0)$, $(0,\pm\pi)$ in the t-t'-J model. This difference is relevant for the nature of the superconducting order parameter,[19] which is a two-component complex quantity for $(\pm\pi/2,\pm\pi/2)$ and more conventional for $(\pm\pi,0)$, $(0,\pm\pi)$. A further difference between the t-J and t-t'-J models is shown in the anisotropy of the effective mass tensor $(m^*/m)_{\mathbf{K}=\mathbf{K}_{\min}}$. The mass tensor is rather anisotropic for the t-J model and nearly isotropic for the t-t'-J model in the U range where the hole pockets are at different positions.

We also investigated the question of hole clustering in the t-J model. Only for large values of J did we find evidence for possible phase separation. For $U\gg t$ and/or a moderate long-range Coulomb interaction $V_{ij}>0$, phase separation is destroyed rapidly. Further results on the thermodynamics of finite clusters[60] indicate that phase separation can be destroyed by particle fluctuations.

In the limit $U=\infty$ we examined the spin structure of the ground state of the 18-site cluster and found, as did Riera and Young,[14] an oscillatory behavior of the ground state S with N_h. This we could connect to the point group symmetry of the ground-state wave function. At quarter-filling the ground state is ferromagnetic with $S=S_{\max}$.

ACKNOWLEDGMENTS

One of us (H.R.) would like to thank S. A. Trugman for valuable discussions. We thank the Leibniz Rechenzentrum München for the generous granting of computer time, and also the HLRZ, c/o KFA Jülich, where parts of the calculations have been performed within the HTC project and under Project No. hbt032.

*Also at Theoretical Division, Los Alamos National Laboratory, Los Alamos, NM 87545

[1]J. G. Bednorz and K. A. Müller, Z. Phys. B **64**, 198 (1986).
[2]R. J. Birgenau and G. Shirane, in *Physical Properties of High Temperature Superconductors,* edited by D. M. Ginsberg (World Scientific, Singapore, 1989).
[3]T. M. Rice, Phys. Scr. **T29**, 72 (1989).
[4]T. M. Rice, J. Less-Comon Met. **164-165**, 1439 (1989).
[5]P. W. Anderson, Science **235**, 1196 (1987).
[6]J. E. Hirsch, Phys. Rev. Lett. **54**, 1317 (1985).

[7]C. Gros, R. Joynt, and T. M. Rice, Phys. Rev. B **36**, 381 (1987).
[8]A. E. Ruckenstein, P. J. Hirschfeld, and J. Appel, Phys. Rev. B **36**, 857 (1987); Z. Zou and P. W. Anderson, *ibid.* **37**, 627 (1988); G. Kotliar and J. Liu, Phys. Rev. Lett. **61**, 1784 (1988); A. Auerbach and D. P. Arovas, *ibid.* **61**, 617 (1988); D. Yoshioka, J. Phys. Soc. Jpn. **58**, 1516 (1989); G. Kotliar and A. E. Ruckenstein, Phys. Rev. Lett. **57**, 1362 (1986).
[9]E. Kaxiras and E. Manousakis, Phys. Rev. B **37**, 656 (1988).
[10]S. A. Trugman, Phys. Rev. B **37**, 1597 (1988).
[11]J. Bonca, P. Prelovsek, and I. Sega, Phys. Rev. B **39**, 7074 (1989).
[12]M. Ogata and H. Shiba, J. Phys. Soc. Jpn. **58**, 2836 (1989).
[13]Y. Hasegawa and D. Poilblanc, Phys. Rev. B **40**, 9035 (1989).
[14]J. A. Riera and A. P. Young, Phys. Rev. B **40**, 5285 (1989).
[15]V. Elser, D. A. Huse, B. I. Shraiman, and E. D. Siggia, Phys. Rev. B **41**, 6715 (1990).
[16]T. Itoh, M. Arai, and T. Fujiwara, Phys. Rev. B **42**, 4834 (1990).
[17]A. Moreo, D. J. Scalapino, R. L. Sugar, S. R. White, and E. Bickers, Phys Rev. B **41**, 2313 (1990).
[18]L. Lilly, A. Muramatsu, and W. Hanke, Phys. Rev. Lett. **65**, 1379 (1990).
[19]J. R. Schrieffer, X. G. Wen, and S. C. Zhang, Phys. Rev. B **39**, 11 663 (1989).
[20]D. Poilblanc and E. Dagotto, Phys. Rev. B **42**, 4861 (1990).
[21]D. Foerster, Z. Phys. B **74**, 295 (1989).
[22]V. J. Emery, S. A. Kivelson, and H. Q. Lin, Phys. Rev. Lett. **64**, 475 (1990).
[23]P. B. Visscher, Phys. Rev. B **10**, 943 (1974).
[24]M. Marder, N. Papanicolaou, and G. C. Psaltakis, Phys. Rev. B **41**, 6920 (1990).
[25]S. G. Ovchinnikov and I. S. Sandalov, Physica B+C **166C**, 197 (1990).
[26]H. Fehske, V. Waas, H. Röder, and H. Büttner, Solid State Commun. **76**, 1333 (1990).
[27]A. R. Bishop, F. Guinea, P. S. Lomdahl, E. Louis, and J. A. Vergés, Europhys. Lett. **14**, 157 (1991).
[28]M. Kato, K. Machida, H. Nakanishi, and M. Fujita, J. Phys. Soc. Jpn. **59**, 1047 (1990).
[29]N. F. Mott, Proc. Phys. Soc. A **62**, 416 (1949).
[30]L. B. Ioffe and G. Kotliar, Phys. Rev. B **42**, 10 348 (1990).
[31]A. Barbieri, J. A. Riera, and A. P. Young, Phys. Rev. B **41**, 11 697 (1990).
[32]B. Doucot and X. G. Wen, Phys. Rev. B **40**, 2719 (1989).
[33]B. S. Shastry, H. R. Krishnamurthy, and P. W. Anderson, Phys. Rev. B **41**, 2375 (1990).
[34]C. Zhou and C. D. Gong, Physica C **169**, 245 (1990).
[35]A. H. MacDonald, S. M. Girvin, and D. Yoshioka, Phys. Rev. B **37**, 9753 (1988).
[36]P. W. Anderson, Phys. Rev. **115**, 2 (1959).
[37]P. Horsch, Helv. Phys. Acta **63**, 345 (1990).
[38]M. S. Hybertsen, E. Stechel, M. Schluter, and D. R. Jennison, Phys. Rev. B **41**, 11 068 (1990).
[39]V. J. Emery, Phys. Rev. Lett. **58**, 2794 (1987).
[40]F. C. Zhang and T. M. Rice, Phys. Rev. B **37**, 3759 (1988).
[41]V. J. Emery and G. Reiter, Phys. Rev. B **38**, 11 938 (1988); F. C. Zhang and T. M. Rice, *ibid.* **41**, 7243 (1990); V. J. Emery and G. Reiter, *ibid.* **41**, 7247 (1990).
[42]M. Uchinami, Phys. Rev. B **42**, 10 178 (1990).
[43]The crucial points here are finite hole concentrations in the thermodynamic limit.
[44]Y. Nagaoka, Phys. Rev. **147**, 392 (1966).
[45]S. A. Trugman, Phys. Rev. B **42**, 6612 (1990); G. S. Tian, J. Phys. A **24**, 513 (1991).
[46]A. Mistriotis, H. Büttner, and W. Pesch, J. Phys. C **21**, L1021 (1988); J. Phys. Condens. Matter **1**, 891 (1989); W. Pesch, H. Büttner, and J. Reichl, Phys. Rev. B **37**, 5887 (1988).
[47]H. Röder, V. Waas, H. Fehske, and H. Büttner, Phys. Rev. B **43**, 6284 (1991). The authors have to comment that the ground-state energies given for the t-t'-J model at various V in Tables I and II of this reference are values per hole N_h. Unfortunately, the divisor N_h was omitted in the head of these tables.
[48]J. A. Riera, Phys. Rev. B **43**, 3681 (1991).
[49]E. Dagotto and A. Moreo, Phys. Rev. D **31**, 865 (1985).
[50]J. K. Cullum and R. A. Willoughby, *Lanczos Algorithms for Large Symmetric Eigenvalue Computations* (Birkhäuser, Boston, 1985).
[51]V. A. Sherman, Solid State Commun. **76**, 321 (1990).
[52]S. A. Trugman, Phys. Rev. B **41**, 892 (1990).
[53]E. Dagotto, A. Moreo, R. Joynt, S. Bacci, and E. Gagliano, Phys. Rev. B **41**, 2585 (1990).
[54]K. V. Szczepanski, P. Horsch, W. Stephan, and M. Ziegler, Phys. Rev. B **41**, 2017 (1990).
[55]R. Eder, K. W. Becker, and W. H. Stephan, Z. Phys. B **81**, 33 (1990).
[56]C. X. Chen and H. B. Schüttler, Phys. Rev. B **41**, 8702 (1990).
[57]X. Zotos, P. Prelovsek, and I. Sega, Phys. Rev. B **42**, 8445 (1990).
[58]J. A. Riera and A. P. Young, Phys. Rev. B **39**, 9697 (1990).
[59]M. Ogata, M. Luchini, S. Sorella, and F. F. Assaad, Phys. Rev. Lett. **66**, 2388 (1991).
[60]H. Röder, H. Fehske, V. Waas, and H. Büttner (unpublished).
[61]J. Kanamori, Prog. Theor. Phys. **30**, 275 (1963).